

F. Vimeux · V. Masson · J. Jouzel · J. R. Petit
E. J. Steig · M. Stievenard · R. Vaikmaa
J. W. C. White

Holocene hydrological cycle changes in the Southern Hemisphere documented in East Antarctic deuterium excess records

Received: 7 July 1999 / Accepted: 21 July 2000

Abstract Four Holocene-long East Antarctic deuterium excess records are used to study past changes of the hydrological cycle in the Southern Hemisphere. We combine simple and complex isotopic models to quantify the relationships between Antarctic deuterium excess fluctuations and the sea surface temperature (SST) integrated over the moisture source areas for Antarctic snow. The common deuterium excess increasing trend during the first half of the Holocene is therefore interpreted in terms of a warming of the average ocean moisture source regions over this time. Available Southern Hemisphere SST records exhibit opposite trends at low latitudes (warming) and at high latitudes (cooling) during the Holocene. The agreement between the Antarctic deuterium excess and low-latitude SST trends supports the idea that the tropics dominate in providing moisture for Antarctic precipitation. The opposite trends in SSTs at low and high latitudes can potentially be explained by the decreasing obliquity during the Holocene inducing opposite trends in the local mean annual insolation between low and high latitudes. It also implies an increased latitudinal

insolation gradient that in turn can maintain a stronger atmospheric circulation transporting more tropical moisture to Antarctica. This mechanism is supported by results from a mid-Holocene climate simulation performed using a coupled ocean-atmosphere model.

1 Introduction

Whereas multidecadal climatic fluctuations during the Holocene are well documented by numerous continental and marine proxies in the Northern Hemisphere (O'Brien et al. 1995; Bond et al. 1997; Mann et al. 1998), there are only a few such records for southern locations (Ciais et al. 1992). The recent warming trend observed in the Southern Hemisphere during the last few decades (Jacka and Budd 1998) highlights the importance of studying Holocene climate variability in this hemisphere. Antarctic ice cores have already provided a wealth of paleoclimatic information including high-latitude temperature records inferred from stable isotopes in ice (either deuterium, δD or oxygen 18, $\delta^{18}O$, measurements) with a focus on glacial-interglacial changes (see Dome F Ice Core Research Group 1998; Steig et al. 1998; Petit et al. 1999 for most recent examples). The combined measurement of these two isotopes can also be used to obtain a complementary paleoclimatic record, deuterium excess which provides information on remote changes in the Southern Ocean (Vimeux et al. 1999 and references therein). We present a series of four Antarctic deuterium excess records covering the Holocene period.

The deuterium excess (d) in precipitation has been defined by Dansgaard (1964) from the meteoric water line (Craig 1961) as follows:

$$d = \delta D - 8\delta^{18}O$$

This isotopic parameter mainly reflects the kinetic fractionation occurring during non-equilibrium fractionation processes such as evaporation above the ocean (Merlivat and Jouzel 1979). Both Rayleigh-type

F. Vimeux (✉) · V. Masson · J. Jouzel · M. Stievenard
Laboratoire des Sciences du Climat et de l'Environnement (LSCE),
UMR CEA-CNRS 1572, Orme des Merisiers, CEA Saclay,
91191 Gif-sur-Yvette cedex, France

J. R. Petit
Laboratoire de Glaciologie et Géophysique de l'Environnement
(LGGE), CNRS, B.P 96, Domaine Universitaire,
38402 Saint Martin d'Hères cedex, France

E. J. Steig
Department of Earth and Environmental Science,
251 Hayden Hall, University of Pennsylvania, Philadelphia,
PA 19104-6316, USA

R. Vaikmaa
Institute of Geology, Tallinn Technical University,
7 Estonia Blvd., 10143 Tallinn, Estonia

J. W. C. White
Institute of Arctic and Alpine Research (INSTAAR),
University of Colorado, Boulder, CO 80309, USA

(Johnsen et al. 1989) and general circulation models (Armengaud et al. 1998; Delaygue 2000) show a positive correlation between the deuterium excess in the vapour above the ocean and the evaporative ocean surface temperature. This correlation results from the dependency of the fractionation processes associated with evaporation on oceanic and meteorological moisture source characteristics (mainly the sea surface temperature, SST, and to a smaller extent the relative humidity of the air just above the sea surface, h). This initial information is partly preserved along the poleward air mass trajectory in spite of the kinetic effects associated with cloud reevaporation and snow formation (Jouzel and Merlivat 1984). These modelling studies support the use of the deuterium excess variations in polar snow as a proxy for fluctuations of the oceanic surface conditions.

Previous studies of deuterium excess in Antarctica have focused on the present-day geographical patterns (Petit et al. 1991; Dahe et al. 1994), on the seasonal cycle (Ciais et al. 1995; Delmotte et al. 2000) and on glacial-interglacial time scales (Jouzel et al. 1982; Vimeux et al. 1999). Here, we discuss Holocene deuterium excess profiles measured with a temporal resolution varying from 20 to 50 years in four cores collected in East Antarctica (Fig. 1 and Table 1), at central locations (Vostok, Dome B and Dome C) and close to the Ross Sea coast (Taylor Dome). The deuterium profiles (proxies for local temperature changes) are discussed and compared with other Antarctic records in a parallel paper (Masson et al. 2000). The advantage of having four cores lies in the possibility of extracting a reliable common deuterium excess from the regional variability. We discuss the trends and variability of the deuterium

excess records and compare them with available ocean surface temperature records in the Southern Hemisphere. We infer that the Holocene Antarctic deuterium excess record largely reflects SST changes at low and mid latitudes and propose a mechanism to account for long term trends.

2 Results

2.1 Deuterium excess records: long term trend during the past 12 ka

2.1.1 Data

The deuterium excess records, presented back to 12 ka along with deuterium records (Fig. 2), exhibit a common long-term trend: they increase steadily during the first half of the Holocene and stabilize between 7 and 6 ka BP (Before Present). Moreover, Vostok and Dome B profiles show a slight increase from 4 ka BP to the present-day. The increasing trend starts during the deglaciation (Jouzel et al. 1982; Vimeux et al. 1999). We focus here on the Holocene period for which the four records are available at a comparable resolution.

Differences in modern deuterium excess values between the different sites can be explained by a continental effect: the deuterium excess increases inland as the $\delta^{18}\text{O}$ - δD slope decreases with the local temperature (Vimeux 1999). We thus compare only deuterium excess deviations from modern values.

The trend at the central sites is larger over the entire Holocene period (3–4‰) than at Taylor Dome (2–3‰), which is the only near-coastal site in this study. The origin of this disparity, which is not related to measurement uncertainties which are of the order of 1‰ for individual deuterium excess determinations (see legend of Fig. 2), is discussed in Sect. 3.

2.1.2 Common signal

A significant common deuterium excess signal has been extracted using the empirical orthogonal function (EOF) analysis. For the three inland sites, the first eigenvector of the deuterium excess time series, smoothed on a 400-year running period, accounts for 66% of the variance (Fig. 3). When the Taylor Dome is included in the principal component analysis (Fig. 3), the first eigenvector still explains 60% of the variance; although the high-frequency variability of the stacked signal is largely influenced by the large amplitude of the fluctuations in the Taylor Dome signal.

By using a multi taper method – singular spectral analysis (MTM-SSA) (Dettinger et al. 1995), we have separated the trend and the high frequency of each EOF (principal component 1, PC 1 and principal component 2–3, PC 2–3 respectively, see legend of Fig. 3). This analysis confirms that while the central sites and the

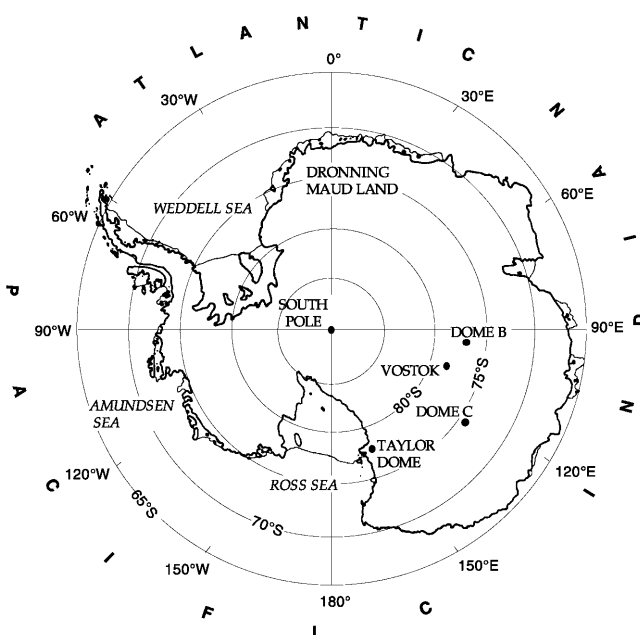


Fig. 1 Map of Antarctica with the locations of each drilling site: Vostok, Dome B, Dome C and Taylor Dome

Table 1 Characteristics of the drilling sites (location, elevation, mean annual temperature, accumulation, sampling, dating): Vostok, Dome B, Dome C and Taylor Dome

	Vostok	Dome B	Dome C	Taylor Dome
Location	78°28'S; 106°48'E	77°05'S; 94°55'E	74°39'S; 124°10'E	77°48'S; 158°43'E
Elevation (m)	3490	3650	3240	2365
Mean annual temperature (°C)	-55.5	-57.5	-53.5	-43.0
Accumulation ($\text{g} \cdot \text{cm}^{-2} \cdot \text{yr}^{-1}$)	2.3	3.8	3.4	5.0 to 7.0
Sampling for isotopes (m)	0.5	1	2	0.5
Time scale	Ice flow model 2D Marine control points	Ice flow model 1D Control points with Byrd dust	Ice flow model 1D Control points with Vostok ^{10}Be	Ice flow model 2D CH4 control points
References	Jouzel et al. (1996) Petit et al. (1999)	Jouzel et al. (1989) Jouzel et al. (1995)	Lorius et al. (1979) Jouzel et al. (1982)	Morse (1997) Morse et al. (1999) Steig et al. (1998)

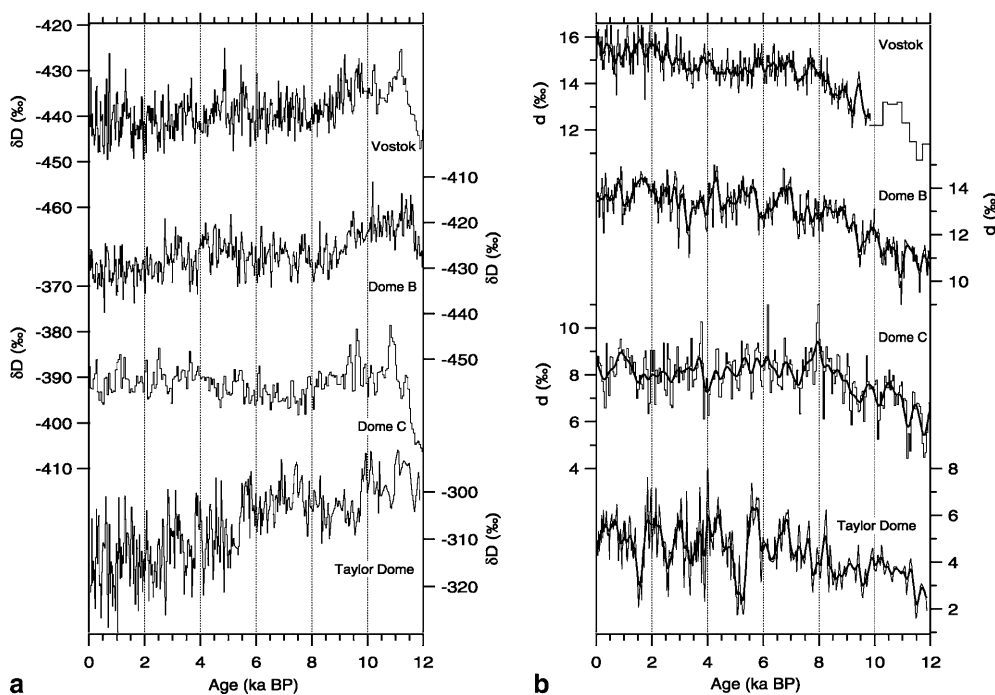


Fig. 2 a Deuterium and b deuterium excess profiles (versus SMOW in ‰) over the last 12 ka [The deuterium excess records are plotted with initial sampling (*thin curves*) along with a 400-year running average (*bold curve*). Due to different depth sampling (see Table 1), the Dome C records have been sampled at 50 year temporal resolution whereas all the other data have been sampled at a 20 year temporal resolution. Each record is presented with its own chronology (see Table 1); the so-introduced lag and lead are smaller than ± 0.5 ka. Dome C records were published in Jouzel et al. (1982). The unpublished isotopic profiles for Vostok and Dome B were measured at the Laboratoire des Sciences du Climat et de l'Environnement (LSCE) and Taylor Dome analyses were performed at the Institute of Arctic and Alpine

Research (INSTAAR, University of Colorado). The accuracy of deuterium excess calculations differs for each profile: $\pm 1.6\text{‰}$ ($\pm 1\text{‰}$ on δD and $\pm 0.15\text{‰}$ on $\delta^{18}\text{O}$) for Dome C, $\pm 1\text{‰}$ ($\pm 1\text{‰}$ on δD and $\pm 0.03\text{‰}$ on $\delta^{18}\text{O}$) for Taylor Dome, and $\pm 0.7\text{‰}$ ($\pm 0.5\text{‰}$ on δD and $\pm 0.05\text{‰}$ on $\delta^{18}\text{O}$) for both Vostok and Dome B. Over the past 10 ka, the Vostok records have been obtained by combining measurements from two shallow cores (BH7 and BH8) after adjusting the two cores depths according to the common ash layer at 102.12 m for BH7 and 101.80 m for BH8. From 12 to 10 ka, both Vostok profiles have been completed with available measurements (Petit et al. 1999 for deuterium with a depth resolution of 1 m *dotted line*; Vimeux et al. 1999 for deuterium excess with a depth resolution of 5 m *dotted line*

Taylor Dome have a common long-term climate trend, the high-frequency information is specific to each site and could be related to local climatic variability (influence of the Ross Ice Shelf for Taylor Dome for instance).

To conclude, these analyses support the use of these deuterium excess records to reconstruct a common oceanic source information on long term trends. We will discuss now the high-frequency variability.

2.2 High frequency variability: signal or noise?

In all the deuterium excess profiles, the long-term trend is punctuated by abrupt and rapid centennial scale events. Such rapid deuterium excess fluctuations may reflect climatic changes or result from deposition and post-deposition processes. First, we propose to examine the variability of the deuterium excess signal through the spectral properties of the four records.

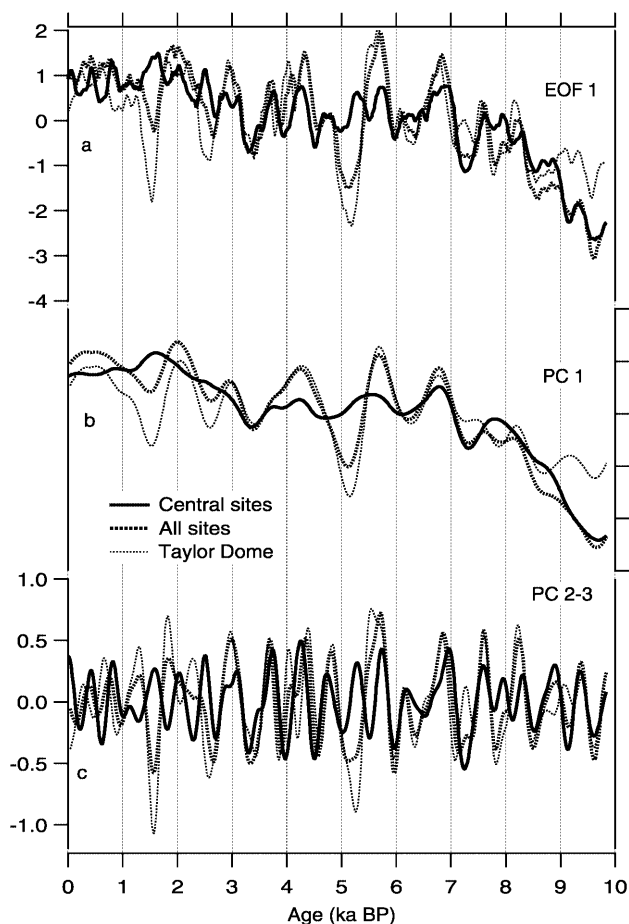


Fig. 3 **a** First EOF (*EOF 1*) computed from a principal component analysis based on the three central Antarctica deuterium excess series and accounting for 66% of the total variance (*bold solid curve*) and on all the sites and representing 60% of the total variance (*bold dotted curve*). Taylor Dome profile is superimposed for comparison (*light dotted curve*). **b** First principal component obtained with MTM-SSA analysis on both *EOF 1* and on Taylor Dome signal (*PC 1*). **c** Second and third principal component obtained with MTM-SSA analysis on both *EOF 1* and on Taylor Dome signal (*PC 2-3*). Calculations have been made on data smoothed with 400-year running average

2.2.1 Spectral analysis

In order to evaluate the spectral properties of the deuterium excess signals, a multi taper method (MTM; Dettinger et al. 1995) has been used with a bandwidth parameter of 4 and 7 tapers (Thomson 1982). We have used the MTM method to compare the power spectra with a red noise spectrum, and to calculate a 90%-confidence level.

Only the Taylor Dome deuterium excess shows a significant periodicity in low frequency mode (periodicities larger than 500 years), at about 930 years (Fig. 4). The millennial scale Taylor Dome periodicity may arise from its coastal location (Ross Sea sector), where ocean/ice-shelf interactions may generate long-term oscillations such as those observed in North Atlantic sediments (Bond et al. 1997; Bianchi and Mc Cave 1999). This periodicity could also reflect a particular climate

oscillation in the Pacific ocean as the Taylor Dome has a higher contribution of Pacific moisture than the central sites, mainly under the influence of the Indian ocean (see Sect. 4.1).

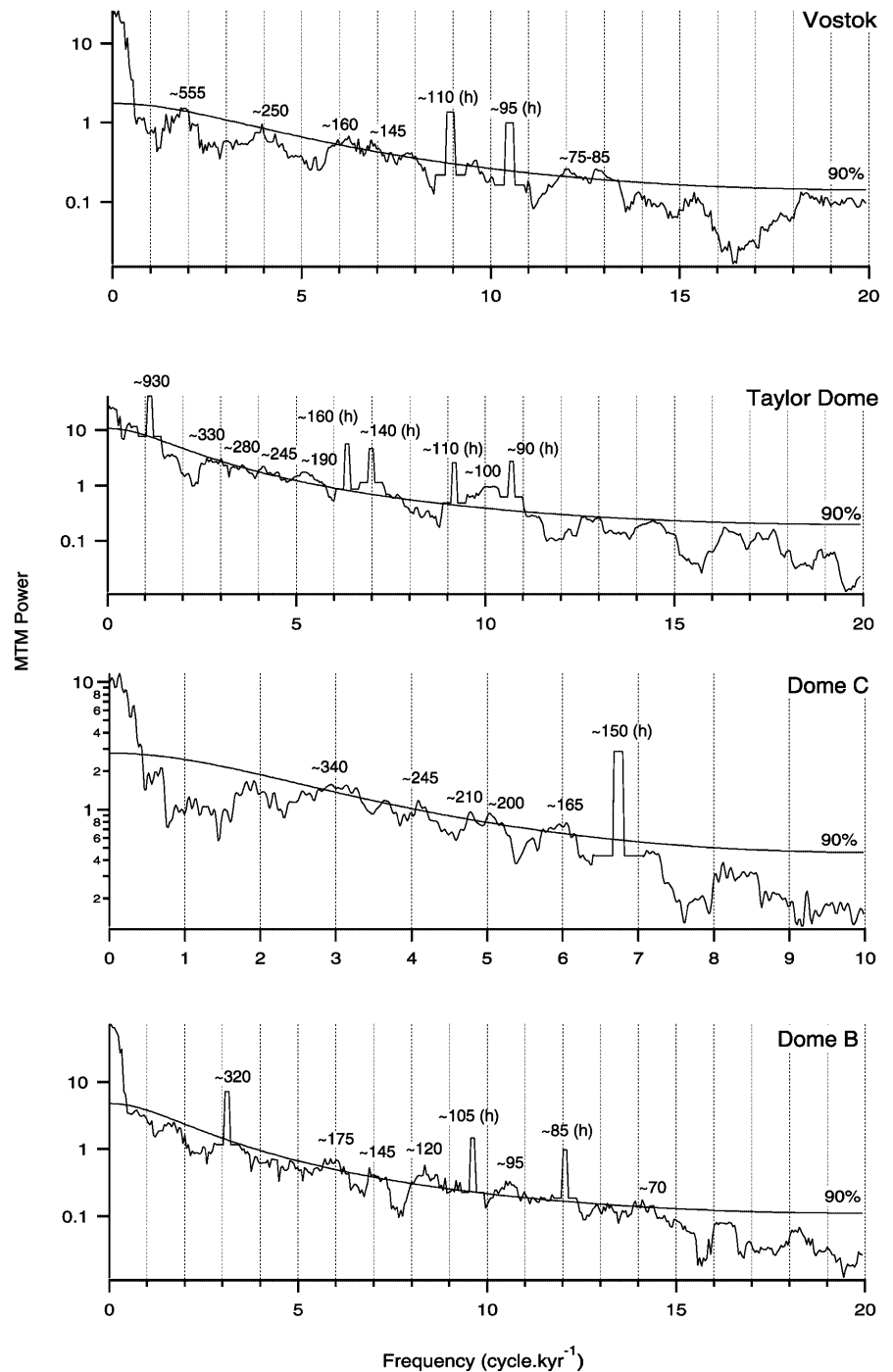
All the records exhibit a range of significant periodicities between 200 and 550 years; however, these frequencies are not robust to changes in the MTM parameters and are not systematically detected by other spectral analysis methods. In the high-frequency band (periodicities lower than 200 years), all sites show a range of common periodicities at multidecadal time scales: 140 to 200 years and 70 to 110 years, the latter not being detected in Dome C due to its lower temporal resolution (Fig. 4). These periods have been documented in high-resolution data from both hemispheres (Stocker and Mysack 1992; Mann et al. 1995; Lamy et al. 1999), commonly attributed to instabilities of the thermohaline circulation. Nevertheless, the uncertainty concerning the glaciological time scales (accuracy of the dating evaluated to 5% at 10 ka) makes the interpretation of such common periodicities delicate. Thus, to test the robustness of these frequencies, we performed the MTM method on Vostok record after correcting the dating as suggested by Blunier et al. (1998): the new power spectrum still shows similar multidecadal period distribution, slightly shifted towards higher periods by less than 10 years in the given range of periodicities (not shown).

2.2.2 Possible mechanisms for high-frequency deuterium excess fluctuations

Although common spectral properties have been detected as described in the previous section, no common rapid shifts can be identified in the different deuterium excess records. The high variability in deuterium excess records may result from: (1) different moisture sources (impact of local sources superimposed on the long-term variability); (2) deposition of the snow (wind scouring, surface micro topography) and (3) post-deposition effects (summer sublimation, depth hoar formation) enhanced by the weak annual accumulation (less than 10 cm of ice equivalent per year for present-day). We discuss those three possible explanations.

Vostok and Dome B are geographically close (300 km apart) but show different deuterium excess variations. The possibility that differences in these two deuterium excess records reflect differences in the origin of the precipitation should be considered. From surface snow data obtained along the route of the 1990 International Trans-Antarctica expedition, Dahe et al. (1994) noted that different isotope-temperature regression lines should be used to represent data east and west of Vostok. In addition, isotopic data from recent snow at Dome B and Vostok fall on different distillation lines (Jouzel et al. 1996). While these observations imply that moisture sources for the two sites are somewhat different, the climate at the moisture source regions could vary in parallel at the scale of the Holocene.

Fig. 4 MTM harmonic power spectrum of the each deuterium excess record (bandwidth parameter, $N\Omega$, 4 with 7 tapers). The median and the 90% confidence level calculated from a red noise simulation are also displayed. Frequencies (in years) are labelled to the nearest 5 years. Harmonic peaks detected by the F-Test (Mann and Lees 1996) are also indicated (*h*)



So far, most of the studies dealing with the estimation of the noise induced by deposition mechanisms have been done for only one isotope. For instance, Benoist et al. (1982) determined that two adjacent cores at Dome C are nearly uncorrelated for times shorter than centuries. The noise induced by deposition mechanisms (Fisher et al. 1985) can be evaluated at Vostok where two ice cores (BH7 and BH8) (see legend of Fig. 1) have been combined to obtain the deuterium excess profile. These cores overlap each other over a depth of 28 m from 102 m to 130 m (corresponding to the interval

3500–4800 years BP, with the appropriate dating, see Table 1). With the initial temporal resolution (20 year sampling), the signal-to-noise ratios are of 0.48, 0.56 and 0.70 for deuterium, oxygen and deuterium excess, respectively. The signal-noise ratio is larger than 1 only when periods shorter than 100 years for each individual isotope are cut off and shorter than 60 years for deuterium excess (one core sample is ~20 years except for Dome C ~50 years). This indicates that deuterium excess record is less noisy than individual isotopes for a similar temporal resolution. The signal-noise ratio

(S/B) is defined as following by Fisher et al. 1985: $S/B = (r_{BH7/BH8}) / (1 - r_{BH7/BH8})$ where $r_{BH7/BH8}$ is the cross-correlation coefficient between the two times series involved.

This better agreement for deuterium excess over δD and $\delta^{18}O$ is probably related to the fact that the variability of the deuterium excess between precipitation events is significantly weaker than for either δD or $8\delta^{18}O$. Indeed, recent measurements performed on precipitation collected at Dome C show that the deuterium excess variation between two successive precipitation events is ~ 5 times lower than for either δD or $8\delta^{18}O$ (Vimeux 1999). Similarly, detailed measurements performed on snowpits show that the range of variation may be 5 to 10 times higher for the deuterium (or for $8\delta^{18}O$) than for the deuterium excess (Vimeux 1999). This results from the fact that the deuterium or oxygen 18 content themselves are significantly and similarly affected by the variability of the local temperature. In contrast, the deuterium excess is primarily influenced by the conditions at the moisture source (that is moisture source temperature as opposed to the local temperature), for which the variability is smaller compared to that of the local temperature.

Due to their present low accumulation rates, all the sites are susceptible to sublimation of summer snow at the surface. Depth hoar formation, for example, has been seen at Taylor Dome and Dome C (Alley et al. 1982; Palais et al. 1982; Waddington and Morse 1994). In the firn, depth hoar will be isotopically heavier than vapour because of non-equilibrium fractionation during condensation. Such post-deposition phase changes may contribute to the deuterium excess variability.

To conclude, while decadal to century scale oscillations with similar periods are apparent in the deuterium excess records from all the cores, it does not appear that these variations are coherent across East Antarctica, and so we will only focus our discussion on the long-term increasing trend of the deuterium excess.

3 Quantitative dependency of the deuterium excess on SST

We use a Rayleigh-type model, MCIM (mixed cloud isotopic model, Petit et al. 1991; Ciais et al. 1994) under present-day conditions to quantify the variations of deuterium excess as a function of both ocean surface temperature (T_{source} , in °C) and relative humidity (h , in %). The model simulates the isotopic fractionation along a direct trajectory to the precipitation site prescribed in terms of inversion temperature and sea-level pressure. This model can be tuned to simulate the modern isotopic composition of surface snow after being prescribed the ocean surface initial conditions (SST, relative humidity and wind speed) and the initial isotopic composition of the vapour above the sea surface, estimated from the global closure assumption (Merlivat and Jouzel 1979). In our simulations, the cloud microphysics, like the supersaturation function, are prescribed according to Ciais et al. (1994) and Petit et al. (1991).

Sensitivity studies performed for each site result in the following regressions: (1) for central sites, $\Delta d = 1.2\Delta T_{source} - 0.15\Delta h$ and (2) for Taylor Dome, $\Delta d = 0.7\Delta T_{source} - 0.3\Delta h$ which indicate that

contrary to SST influence, the imprint of relative humidity decreases inland as already noted by Petit et al. (1991). We have not been able to develop a simple physical explanation to account for this result, but it appears to be a robust observation.

In order to compare past fluctuations in deuterium excess with SST records (no indicator of past changes in relative humidity alone is available and complex model simulations show very weak relative humidity changes even between a glacial and modern climates, see Vimeux et al. 1999 and Bush and Philander 1999), we explore the relationship between present-day SST and relative humidity. The saturation vapour pressure relationship is a strong thermodynamical control linking these two variables. Three atmospheric general circulation models (GISS, LMD and EC-HAM, Joussaume and Taylor 1995) show a linear spatial SST-relative humidity relationship over the Southern Hemisphere ocean surface with a common slope of -0.42% per °C in the 7 °C to 24 °C range ($\sigma = \pm 0.04\%$ per °C). Simulations of last glacial maximum climate show that this relationship is preserved for past periods.

Combining this slope with relationships deduced from the MCIM, we obtain a quantitative interpretation of the deuterium excess fluctuations in terms of SST alone: $\Delta d = 1.26\Delta T_{source}$ for central sites and $\Delta d = 0.83\Delta T_{source}$ for Taylor Dome. It is satisfactory to note that these correlations are in good agreement with those given by general circulation models which have the advantage of taking into account a mixture of the different source regions (Delaygue 2000).

Assuming similar moisture sources for Taylor Dome and central sites, similar SST changes should induce different deuterium excess variations. This is indeed the case throughout the Holocene and the ratio of deuterium excess increase at Taylor Dome compared with central sites ($2.5/3.5 = 0.71$) is in good agreement with the ratio of the simulated deuterium excess-SST slopes ($0.83/1.26 = 0.66$).

4 Holocene climate: discussion

4.1 Comparison with SST reconstructions

The general increase in deuterium excess during the first half of the Holocene indicates, according to simple models, an increase of the weighted average temperature of the oceanic moisture sources. This may result either from a general Southern Hemisphere oceanic warming or from a shift of the evaporative sources towards lower latitudes (or to a combination of these two effects). We first determine the oceanic basins providing moisture to our sites before comparing our deuterium excess records with SST reconstructions from those basins.

The main oceanic basin contributing to Antarctic precipitation have been estimated using the NASA/GISS low-resolution atmospheric general circulation model in which five source regions are distinguished: Indian Ocean, Pacific Ocean, Atlantic Ocean, high-latitude ocean (part of each oceanic basin characterized by a seasonal sea-ice cover) and Antarctica (polar moisture recycling). For all of our ice core locations, the main contributor is the Indian Ocean (54, 47, 60 and 40% of annual precipitation for Vostok, Dome B, Dome C and Taylor Dome respectively) and secondly the Pacific Ocean (14, 18, 14 and 33%). We thus focus our comparison on available SST reconstructions from these two oceanic basins.

Two distinct SST behaviours can be distinguished depending on the latitude of the site. At mid and low

latitudes (northward of the subtropical convergence $\sim 40^\circ\text{S}$), SST steadily increases during the first half of the Holocene and then either increases or remains stable until the present day (Schneider et al. 1995; Bard et al. 1997; Beck et al. 1997; Claire Waelbroeck personal communication); some of these curves are presented in Fig. 5. Based on the alkenone method, the associated warming is estimated to reach 1 to 3 °C over the last 12 ka (Table 2 and Fig. 5).

In contrast, the few SST records located at high latitudes (south of 45°S) covering the Holocene are characterized by an early Holocene optimum (around 10–12 ka) and a significant decreasing trend since 6 ka BP (Salvignac 1998; Claire Waelbroeck personal communication), as measured using planktonic species counts associated with the modern analogue technique (Table 2). Note that two different SST reconstruction methodologies are used at low and high latitudes (alkenones in coccoliths versus foraminiferal species distributions). Although a quantitative comparison between absolute temperature obtained by these different methods is difficult (because of different seasonality and living depths), general trends can be compared.

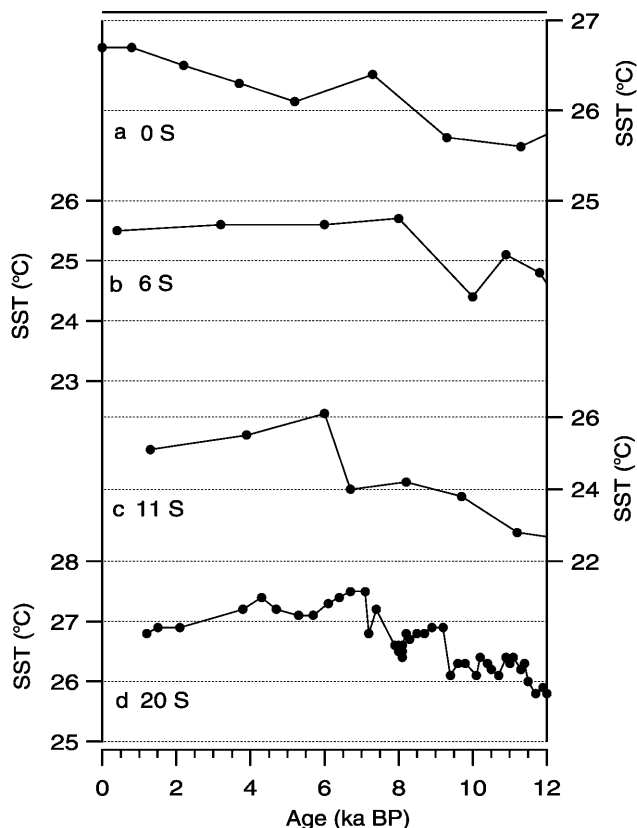


Fig. 5a–d SST reconstructions from Indian Ocean at low latitudes between 0°S and 20°S ; **a** and **d** MD 85668 (0°S) and MD 79257 (20°S) respectively, Bard et al. (1997); **b** and **c** GeoB 1008-3 (6°S) and GeoB 1016-3 (11°S) respectively, Schneider et al. (1995). Both reconstructions are given with the estimated error of $\pm 0.3^\circ\text{C}$

Table 2 Comparison of SST variations during the Holocene for different cores located at low and high latitudes. Temperature deviations are given from 12 ka BP for cores at low latitudes and from the early Holocene temperature optimum for cores at high latitudes (at around 10–11 ka) to describe the general trend of the SST over the Holocene period. Error bars on temperature reconstructions are inferior to $\pm 0.3^\circ\text{C}$ at low latitudes and about $\pm 1.5^\circ\text{C}$ at high latitudes

Cores	6 ka BP SST deviation (°C)	12 ka BP Reference
GeoB 1008-3 (6°S) Schneider et al. (1995)	+1.0	0
GeoB 1016-3 (11°S) Schneider et al. (1995)	+3.4	0
MD 79 257 (20°S) Bard et al. (1997)	+1.5	0
Average value (M)	M = 2.0	$\leftarrow^{+2.0}$ M = 0
		Temperature optimum (~ 10 – 11 ka BP) Reference
MD 80 304 (51°S) Salvignac (1998)	-3.4	\leftarrow 0
MD 80KK63 (52°S) Salvignac (1998)	-3.0	0
Average value (M)	M = -3.2	$\leftarrow^{-3.2}$ M = 0

The general increase of deuterium excess is in good agreement with the SST trend at low and mid latitudes. Moreover, the magnitude of warming is consistent with the SST-based interpretation of Antarctic deuterium excess. Indeed, according to simple models discussed in Sect. 3, a $\sim 3.5\text{‰}$ increase in central Antarctic deuterium excess and a $\sim 2.5\text{‰}$ increase at Taylor Dome are both associated with a source warming of $\sim 2.8^\circ\text{C}$ which is only slightly higher than the values inferred from reconstructed low-latitude temperature series (Table 2). The moisture source is not restricted to the low latitudes and small, but varying, contributions from cold oceans may modulate the weighted source temperature recorded in the deuterium excess record. Moreover, the local temperature effect on the deuterium excess profile can not be discarded and could contribute, to a smaller extent, to this discrepancy (see Sect. 2.1).

In summary, observed changes in deuterium excess reflect the warming of the weighted temperature of sources regions, probably mainly located at mid and low latitudes.

This climatic trend may result from a dynamical process initiated in the deglaciation. It is also possible that the SST trends are only forced by insolation (Pailard 1998). We propose to explore here the influence of the insolation forcing on the response of the hydrological cycle.

In Vimeux et al. (1999) Antarctic deuterium excess fluctuations during the last climatic cycle have been interpreted as the imprint of the changing relative contributions between low and high latitudes to the precipitation, driven by the latitudinal difference of annual mean insolation.

Over the Holocene period, the annual mean insolation shows different trends at latitudes higher and lower than $\sim 45^\circ\text{S}$, and may have contributed to the latitudinal patterns of SST variations. Although the annually averaged changes are small, on the order of 1 W/m^2 , they may produce significant heating or cooling at the sea surface because the upper ocean integrates direct insolation forcing over several years (Cortijo et al. 1999). The annual insolation at high latitudes, in phase with obliquity (Loutre 1993), exhibits an optimum around 10 ka, as does the SST, and decreases by about 1.53 W/m^2 during the Holocene whereas at low latitudes the Holocene trend is toward higher insolation with a change of 0.86 W/m^2 . The resulting increase in latitudinal insolation gradient from 10 ka BP should have enhanced the poleward atmospheric circulation over the course of the Holocene, thus supporting a northward shift of the dominant evaporative source regions during this period.

Therefore, we propose that the average source of Antarctic precipitation moves towards low latitudes as a result of changes in both evaporation (related to SST increase) and efficiency of the poleward atmospheric transport, in response to different latitudinal annual insolation changes. This mechanism is supported by mid-Holocene ocean surface climate changes simulated by a coupled ocean-atmosphere model described later.

4.2 Climate simulation with a coupled ocean-atmosphere model

Two simulations (present-day and mid-Holocene climate, 6 ka ago) have been performed by Braconnot et al. (1997, 2000) using the low-resolution IPSL (Institut Pierre-Simon Laplace) coupled ocean-atmosphere climate model, with no flux correction at the air-sea interface. The control climate is a 150 year simulation of the present day climate and the simulation of the 6 ka climate starts on year 21 of the control simulation and is also 150-years long, without any long term drift. For the 6 ka simulation, the CO_2 level is kept to the value of the control experiment and the only forcing is the change in orbital configuration. We show results obtained by averaging the last 20 years of each simulation.

Figure 6 shows the comparison of the zonal annual mean temperature and evaporation between coupled 6 ka and modern simulations along with the mean annual insolation. Both temperature and evaporation evolve in parallel, reflecting changes in annual insolation. Moreover, a clear feature of the zonal annual difference of these parameters is exhibited at $\sim 40^\circ\text{S}$: below this threshold, 6 ka temperature were lower than now, while they were higher at higher latitudes.

The model shows clearly a great homogeneity between each oceanic basin so that the zonal annual mean is really representative of the global situation. Moreover, the latitudinal temperature gradient is less marked in the seasonal cycle, further confirming that the

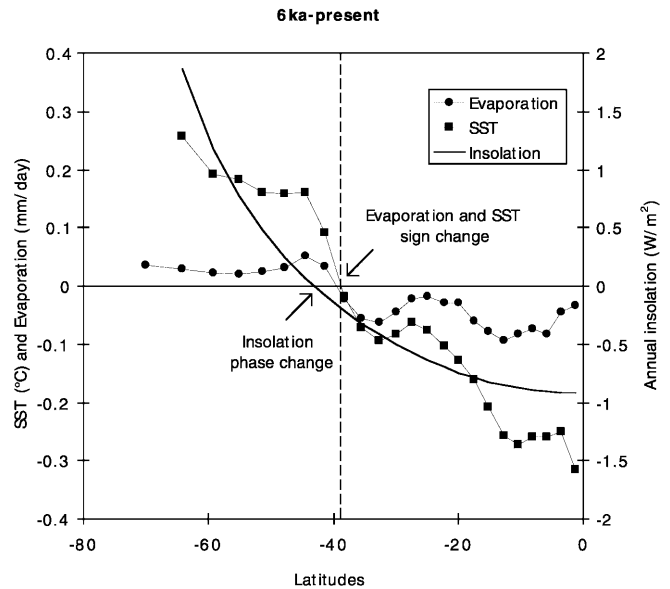


Fig. 6 Zonal mean annual difference between coupled ocean-atmosphere simulations at 6 ka and present-day for evaporation (mm/day), sea surface temperature ($^\circ\text{C}$) and mean annual insolation (W/m^2). The accuracies for sea surface temperature and evaporation are respectively $\pm 0.03 \text{ }^\circ\text{C}$ and $\pm 0.015 \text{ mm/day}$

obliquity changes are involved (not the precession) as already suggested by Mitchell et al. (1988).

To quantify the deuterium excess change, we have run the GISS isotopic model with the SST from the coupled run at 6 ka. The GISS model shows a 1‰ deuterium excess increase between 6 ka and the control run at Vostok, in good agreement with our data. Note that similar simulations with fixed modern SST do not exhibit any variations of the deuterium excess between 6 ka and control run in response to insolation change only.

The model results thus support our interpretation of a northward shift of the evaporative areas during the Holocene associated with an increase of the SST gradient in Southern Hemisphere in response to the obliquity increase.

4.3 Comparison with the Northern Hemisphere

Similarly to the Southern Hemisphere, opposite SST trends at low and high latitudes have also been evidenced during the Holocene in the North Atlantic (Ruddiman and Mix 1993; Kyung and Slowey 1999). Similar SST patterns have been simulated by atmospheric general circulation models coupled with surface ocean models and forced by 9 and 6 ka insolation (Mitchell et al. 1988; Liao et al. 1994). The deuterium excess record in central Greenland (GRIP, not shown) is also characterized by an increasing trend during the Holocene quite similar to that observed in Antarctic records. This good agreement between GRIP and East Antarctic deuterium excess profiles suggest that similar

insolation-induced mechanisms have operated in northern and southern oceans during the Holocene period. A recent study (Cortijo et al. 1999) has also pointed out the great similarity between North Atlantic SST patterns during the Holocene (increase at low latitudes and decrease at high latitudes) and the last interglacial period in response to the latitudinal insolation gradient. The Vostok deuterium excess record (Vimeux et al. 1999), which covers one full climate cycle, also enables the comparison of Holocene and Eemian interglacial stages. During both interglacial periods, the deuterium excess increases markedly reflecting the variations of the relative contribution of low and high latitudes to Antarctic precipitation. Recent deuterium excess results obtained in the Vostok core suggest that the situation was similar during the previous warm periods (Vimeux 1999). Similar behaviour in ocean areas from both hemispheres seems therefore to have taken place during interglacial periods, as a result of parallel insolation gradient changes.

5 Conclusions and perspectives

Four East Antarctic deuterium excess records exhibit a common significant increasing trend over the course of the Holocene that can reasonably be interpreted in terms of a warming of the weighted-average moisture source (2–3 °C). The deuterium excess increasing trend is consistent with SST reconstructions at low and mid latitudes. It appears that the Antarctic evaporative sources have probably gradually moved northward during the course of the Holocene, possibly under the influence of a mechanism involving the increase of the latitudinal annual insolation gradient. This is likely associated with a somewhat more intense equator-to-pole atmospheric transport which explains the increasing contribution of warm source waters to the Antarctic precipitation. This interpretation is supported by results of a mid Holocene climate simulation performed with a coupled ocean-atmosphere climate model. Additional simulations with more extreme orbital configurations (obliquity extrema) would be required to further validate our proposed mechanism. Overall, this detailed study focusing on the Holocene reinforces the interpretation of the Antarctic deuterium excess records in terms of ocean temperature changes (Vimeux et al. 1999).

We have also seen high-frequency fluctuations in deuterium excess records, although it is not clear how these oscillations are related from site to site in East Antarctica. Long present-day climate simulations with coupled climate models including the water isotopic cycle would improve our understanding of the internal oscillations possibly responsible for the multidecadal to century scale isotopic variability (70 to 200 years). If deuterium excess profiles are to be used to detect and document southern ocean climate changes at the century or millennial time scale, further studies of Antarctic

present-day regional meteorological variability (as e.g. between Vostok and Dome B sites) and deposition processes are required. Traverses organized by the ITASE program (International Trans Antarctic Scientific Expeditions) with simultaneous sampling of common precipitation events at different locations would enable us to better understand the impact of regional climate variability on the deuterium excess. In addition, processes such as depth hoar formation, that may cause post-depositional fractionation, should be further investigated by laboratory experiments.

Ongoing deuterium excess measurements along coastal sites (Law Dome) and new drilling sites in the Atlantic sector (Dome F, EPICA Dronning Maud Land) and western Antarctica (Siple Dome) will enable us to study the spatial variability of deuterium excess past fluctuations and the sea-ice influence.

Acknowledgements We warmly thank Pascale Braconnot for providing simulations with the IPSL coupled ocean-atmosphere climate model as well as Gilles Delaygue, Elsa Cortijo, Monique Labracherie and Claire Waelbroeck for fruitful discussions. We are also very grateful to the reviewers and S. Johnsen for their constructive criticisms. This is LSCE contribution n° 497.

References

- Alley RB, Bolzan JF, Whillans I (1982) Polar firn densification and grain growth. *Ann Glaciol* 3: 7–11
- Armengaud A, Koster RD, Jouzel J, Ciais P (1998) Deuterium deuterium excess in Greenland snow: analysis with simple and complex models. *J Geophys Res* 103 (D8): 8947–8953
- Bard E, Rostek F, Sonzogni C (1997) Interhemispheric synchrony of the last deglaciation inferred from alkenone palaeothermometry. *Nature* 385: 707–710
- Beck JW, Recy J, Taylor F, Edwards RL, Cabloch G (1997) Abrupt changes in early Holocene tropical sea surface temperature derived from coral records. *Nature* 385: 705–707
- Benoist JP, Jouzel J, Lorius C, Merlivat L, Pourchet M (1982) Isotope climatic record over the last 2.5 ka from Dome C, Antarctica, Ice cores. *Ann Glaciol* 3: 17–22
- Bianchi G, Mc Cave I (1999) Holocene periodicity in North Atlantic climate and deep-ocean flow south of Iceland. *Nature* 397: 515–517
- Blunier T, Chappellaz J, Schwander J, Dällenbach A, Stauffer B, Stocker TF, Raynaud D, Jouzel J, Clausen HB, Hammer CU, Johnsen SJ (1998) Asynchrony of Antarctic and Greenland climate change during the last glacial period. *Nature* 394: 739–743
- Bond G, Showers W, Cheseby M, Lotti R, Almasi P, deMenocal P, Priore P, Cullen H, Hajdas I, Bonami G (1997) A pervasive millennial-scale cycle in North Atlantic Holocene and glacial climates. *Science* 278: 1257–1266
- Braconnot P, Marti O, Joussaume S (1997) Adjustments and feedbacks in a global coupled ocean-atmosphere model. *Clim Dyn* 13: 507–519
- Braconnot P, Marti O, Joussaume S (2000) Ocean feedback in response to 6 ka BP insolation. *J Clim* 13: 1537–1553
- Bush ABG, Philander SGH (1999) The climate of the Last Glacial Maximum: results from a coupled atmosphere-ocean general circulation model. *J Geophys Res* 104 (D20): 24 509–24 525
- Ciais P, Petit JR, Jouzel J, Lorius C, Barkov N, Lipenkov V, Nicolaev V (1992) Evidence for an early Holocene climatic

- optimum in the Antarctic deep ice-core record. *Clim Dyn* 6: 169–177
- Ciais P, Jouzel J, Petit JR, Lipenkov V, White JWC (1994) Holocene temperature variations inferred from six Antarctic ice cores. *Ann Glaciol* 20: 427–436
- Ciais P, White JWC, Jouzel J, Petit JR (1995) The origin of present-day Antarctic precipitation from surface snow deuterium deuterium excess data. *J Geophys Res* 100 (D9): 18 917–18 927
- Cortijo E, Lehman S, Keigwin L, Chapman M, Paillard D, Labeyrie L (1999) Changes in meridional temperature and salinity gradients in the North Atlantic Ocean (30° to 72°N) during the Last Interglacial period. *Paleoceanography* 14: 23–33
- Craig H (1961) Isotopic variations in meteoric waters. *Science* 133: 1702–1703
- Dahe Q, Petit JR, Jouzel J, Stievenard M (1994) Distribution of stable isotopes in surface snow along the route of the 1990 International Trans-Antarctica Expedition. *J Glaciol* 40: 107–118
- Dansgaard W (1964) Stable isotopes in precipitation. *Tellus* 16: 436–447
- Delaygue (2000) Relations entre surface océanique et composition isotopique des précipitations Antarctiques: simulation pour différents climats. PhD Thesis Université Aix-Marseille 3, Marseille, France
- Delmotte M (1997) Enregistrements climatiques à Law Dome: variabilité pour les périodes récentes et pour la déglaciation. PhD Thesis Université Joseph Fourier, Grenoble, France
- Delmotte M, Masson V, Jouzel J, Morgan V (2000) A seasonal deuterium excess signal at Law Dome, coastal eastern Antarctica: a southern ocean signature. *J Geophys Res* 105(D6): 7187–7197
- Dettinger MD, Ghil M, Strong CM, Weibel W, Yiou P (1995) Software expedites singular-spectrum analyses of noisy time series. *EOS trans. AGU* 76: 12
- Dome F Ice Core Research Group (1998) Preliminary investigation of palaeoclimate signals recorded in the ice core from Dome Fuji station, east Dronning Maud Land. *Ann Glaciol* 27: 338–342
- Fisher D, Reeh N, Clausen HB (1985) Stratigraphic noise in time series derived from ice cores. *Ann Glaciol* 7: 76–83
- Jacka T, Budd W (1998) Detection of temperature and sea-ice extent changes in the Antarctic and Southern Ocean, 1949–96. *Ann Glaciol* 27: 553–559
- Johnsen SJ, Dansgaard W, White JWC (1989) The origin of Arctic precipitation under present and glacial conditions. *Tellus* 41B: 452–468
- Joussame S, Taylor KE (1995) Status of the Paleoclimate Modeling Intercomparison Project (PMIP). In: Gates WL (ed) *Proc 1st Int AMIP Sci Conf*, Monterey, CA. WCRP pp 425–430
- Jouzel J, Merlivat L (1984) Deuterium and oxygen 18 in precipitation: modeling of the isotopic effects during snow formation. *J Geophys Res* 89(D7): 11 749–11 757
- Jouzel J, Merlivat L, Lorius C (1982) Deuterium deuterium excess in an East Antarctic ice core suggests higher relative humidity at the oceanic surface during the last glacial maximum. *Nature* 299: 688–691
- Jouzel J, Raisbeck G, Benoist JP, Yiou F, Lorius C, Raynaud D, Petit JR, Barkov NI, Korotkevitch YS, Kotlyakov V (1989) A comparison of deep Antarctic ice cores and their implications for climate between 65 000 and 15 000 years ago. *Quat Res* 31: 135–150
- Jouzel J, Vaikmae R, Petit JR, Martin M, Duclos Y, Stievenard M, Lorius C, Toots M, Mélières MA, Burckle LH, Barkov NI, Kotlyakov VM (1995) The two-step shape and timing of the last deglaciation in Antarctica. *Clim Dyn* 11: 151–161
- Jouzel J, Waelbroeck C, Malaize B, Bender M, Petit JR, Stievenard M, Barkov NI, Barnola JM, King T, Kotlyakov VM, Lipenkov V, Lorius C, Raynaud D, Ritz C, Sowers T (1996) Climatic interpretation of the recently extended Vostok ice records. *Clim Dyn* 12: 513–521
- Kyung EL, Slowey NC (1999) Cool surface waters of the subtropical North Pacific Ocean during the last glacial. *Nature* 397: 512–514
- Lamy F, Hebbeln D, Wefer G (1999) Holocene climatic change recorded in marine sediments of southern Chile (41°S). *Journal of Conference 4*, European Union of Geosciences 10
- Liao X, Street-Perrott A, Mitchell JFB (1994) GCM experiments with different cloud parametrization: comparisons with palaeoclimatic reconstructions for 6000 years BP. *Paleoclimates* 1: 99–123
- Lorius C, Merlivat L, Jouzel J, Pourchet MA (1979) 30 000-yr isotope climatic record from Antarctic ice. *Nature* 280: 644–648
- Loutre MF (1993) Paramètres orbitaux et cycles diurne et saisonnier des insulations. PhD Thesis Université Catholique de Louvain, Louvain-la-Neuve, Belgium
- Mann ME, Lees JM (1996) Robust estimation of background noise and signal detection in climatic time series. *Clim Change* 33: 409–445
- Mann ME, Park J, Bradley RS (1995) Global interdecadal and century-scale climate oscillations during the past five centuries. *Nature* 378: 266–270
- Mann ME, Bradley RS, Malcolm KH (1998) Global-scale temperature patterns and climate forcing over the past six centuries. *Nature* 392: 779–787
- Masson V, Vimeux F, Jouzel J, Morgan V, Delmotte M, Hammer C, Johnsen SJ, Lipenkov V, Petit JR, Steig E, Stievenard M, Vaikmae R (2000) Holocene temporal and spatial climate variability in Antarctica. *Quat Res* (in press)
- Merlivat L, Jouzel J (1979) Global climatic interpretation of the deuterium-oxygen 18 relationship for precipitation. *J Geophys Res* 84(C8): 5029–5033
- Mitchell JFB, Grahame NS, Needham KJ (1988) Climate simulations for 9000 years before present: seasonal variations and effect of the Laurentide ice sheet. *J Geophys Res* 93(D7): 8283–8303
- Morse DL (1997) Glacier geophysics at Taylor Dome, Antarctica. PhD Thesis, University of Washington, USA
- Morse DL, Waddington ED, Marshall HP, Neumann TA, Steig EJ, Dibb JE, Winebrenner DP, Arthern RJ (2000) Accumulation rate measurements at Taylor Dome, East Antarctica: techniques and strategies for mass balance measurements in polar environments. *Geogr Ann* 81A: 683–694
- O'Brien S, Mayewski P, Meeker L, Meese D, Twickler M, Withlow S (1995) Complexity of Holocene climate as reconstructed from Greenland ice core. *Science* 270: 1962–1964
- Paillard D (1998) The timing of Pleistocene glaciations from a simple multiple-state climate model. *Nature* 391: 378–381
- Palais JM, Whillans IM, Bull C (1982) Snow stratigraphic studies at Dome C, East Antarctica: an investigation of depositional and diagenetic processes. *Ann Glaciol* 3: 239–242
- Petit JR, White JWC, Young NW, Jouzel J, Korotkevich YS (1991) Deuterium excess in recent Antarctic snow. *J Geophys Res* 96(D3): 5113–5122
- Petit JR, Jouzel J, Raynaud D, Barkov NI, Barnola JM, Basile I, Bender M, Chapellaz J, Davis J, Delaygue G, Delmotte M, Kotlyakov VM, Legrand M, Lipenkov V, Lorius C, Pépin L, Ritz C, Saltzman E, Stievenard M (1999) 420 000 years of climate and atmospheric history revealed by the Vostok Deep Antarctic ice Core. *Nature* 399: 429–436
- Ruddiman WF, Mix AC (1993) The north and equatorial Atlantic at 9000 and 6000 yr BP. In: Wright HEJ, Kutzbach JE, Webb TW III, Ruddiman WF, Street-Perrott FA, Bartlein PJE (eds) *Global climates since the Last Glacial Maximum*. University of Minnesota Press, Minneapolis, USA, pp 94–124
- Salvignac ME (1998) Variabilité hydrologique et climatique dans l'Océan Austral (secteur indien) au cours du Quaternaire terminal. Essai de corrélations inter-hémisphériques. PhD Thesis, Université de Bordeaux 1, Bordeaux, France
- Schneider RR, Müller PJ, Ruhland G (1995) Late quaternary surface circulation in the east equatorial South Atlantic: evidence from alkenone sea surface temperatures. *Paleoceanography* 10: 197–219

- Steig EJ, Brook EJ, White JWC, Sucher CM, Bender ML, Lehman SJ, Morse DL, Waddington ED, Clow GD (1998) Synchronous climate changes in Antarctica and the North Atlantic. *Science* 282: 92–95
- Stocker TF, Mysack LA (1992) Climatic fluctuations on the century time-scale: a review of high resolution proxy data and possible mechanisms. *Clim Change* 20: 227–250
- Thomson DJ (1982) Spectrum estimation and harmonic analysis. *Proc. IEEE* 70, pp 1055–1096
- Vimeux F (1999) Variations de l'excès en deutérium en Antarctique au cours des 400 000 dernières années: implications climatiques. PhD Thesis Université Paris 7-Denis Diderot, Paris, France
- Vimeux F, Masson V, Jouzel J, Stievenard M, Petit JR (1999) Glacial-interglacial changes in ocean surface conditions in the Southern Hemisphere. *Nature* 398: 410–413
- Waddington ED, Morse DL (1994) Spatial variations of local climate at Taylor Dome, Antarctica: implications for paleoclimate from ice cores. *Ann Glaciol* 20: 219–225